Characteristics of wave induced oscillations in mesospheric O$_2$ emission intensity and temperatures

A. Taori

Aryabhatta Research Institute of Observational Sciences (ARIES), Nainital, India

M. Taylor

Center for Atmospheric and Space Science, Utah State University, Logan, Utah, USA

[1] Gravity wave and tidal signatures in mesospheric emissions can be characterized using a quantity η which relates the wave intensity perturbations to the corresponding induced temperature oscillation. The quasi-monochromatic wave induced oscillations in the O$_2$ (0−1) atmospheric emission observed from Maui, Hawaii (20.8 N, 156.2 W) have been investigated for the periods ranging from 1–12 hours. Our results clearly show that $|\eta|$ increases from 0.5 to 10 with the increasing wave periods while the phase Ø exhibits a decreasing trend (+75 to −100°). When compared with model, observed trends agree well while significant differences in the absolute values are noted, possibly due to complex chemical and dynamical processes at mesospheric altitudes. **Citation:** Taori, A., and M. Taylor (2006), Characteristics of wave induced oscillations in mesospheric O$_2$ emission intensity and temperatures, *Geophys. Res. Lett.*, *33*, L01813, doi:10.1029/2005GL024442.

1. Introduction

[2] It is now well understood that temporal variations of the airglow emission intensities and temperatures are dominated by the passage of gravity wave and tides through the ∼80−100 km region [e.g., *Takahashi et al.*, 1985; *Taylor et al.*, 1987]. *Krassovsky* [1972] introduced a parameter, termed η for quantifying the hydroxyl (OH) emission perturbations which relates the percentage intensity changes to the associated temperature variations. Originally, η was defined as a simple parameter but recent modeling studies have shown that the interaction between the chemical and dynamical processes for different wave periodicities is a complex parameter of the form $\eta = |\eta| \, e^{i\varnothing}$ where, Ø denotes the phase difference between intensity and temperature oscillation. Several modeling studies have since been performed to investigate the interaction of gravity waves, mainly with the OH airglow emission [*Tarasick and Shepherd*, 1992a, 1992b; *Hickey et al.*, 1993; *Walterscheid and Schubert*, 1995, and references therein]. However, observational evidence of the magnitude and phase of η over a range of wave periodicities is still very limited. Most notable observations of η for the OH emission have been performed by *Viereck and Deehr* [1989] spanning the wave period range of ∼1−20 hrs, and by *Reisin and Scheer* [1996] who focused mainly on semidiurnal tidal fluctuations. Other limited data for isolated quasi-monochromatic wave events have been described by *Takahashi et al.* [1992] and *Taylor et al.* [2001]. In comparison, studies of η for the O$_2$ (0−1) Atmospheric band emission are significantly fewer [*Viereck and Deehr*, 1989; *Hecht and Walterscheid*, 1991; *Takahashi et al.*, 1992; *Reisin and Scheer*, 1996; *Zhang et al.*, 1993]. Taken together, these data represent significant progress but an incomplete picture for the distribution of η (amplitude as well as phase) with the range of wave periodicity.

[3] This paper reports novel near simultaneous measurements of η in the NIR O$_2$ (0−1) band at low-latitudes using the CEDAR Mesospheric Temperature Mapper (MTM). Measurements were obtained for discrete wave periods ranging from ∼1 to 12 hours during the winter time in 2002−2004. The results are compared directly with existing data in the literature and model results.

2. Observations and Results

[4] The MTM is a high performance imaging system that utilizes a large format (6.45 cm^2), 1024 × 1024 pixel CCD array coupled to a 90° circular field of view telecentric lens system. The high quantum efficiency (∼50% at near IR wavelengths) and low noise characteristics (dark ∼0.1 e$^-$/pixel/sec at −50°C) of the CCD array provide capability of high quality nocturnal measurements of OH and O$_2$ emission intensity (precision <0.5% in 1 minute) and derived rotational temperatures (precision <1−2 K in 3 minutes) using similar methods as of *Reisin and Scheer* [1996]. Details of the instrument are discussed elsewhere [*Taylor et al.*, 2001].

[5] Since the deployment of MTM in November 2001 at the air force AEOS facility, Maui (20.8N, 156.2W), routine measurements of NIR OH (6−2) Meinel band and O$_2$ (0−1) Atmospheric band emission has been conducted. A wealth of coherent wave structures are detected in both the emissions, however, the OH emission is subject to a severe chemical decay processes resulting fast intensities decay in the evening hours [*Lowe et al.*, 1996] which can significantly affect the determination of wave periodicity (for long period events). Therefore, we have limited our analysis to O$_2$ (0−1) data set and have focused on wave periodicities in the range of ∼1−12 hrs.

[6] Figure 1 shows two examples illustrating variability observed in the O$_2$ (0−1) band emission data during the course of a night. The data were recorded in December 2002 (UT day 337) and January 2003 (UT day 003). In the December data (left panel) a general upward trend in
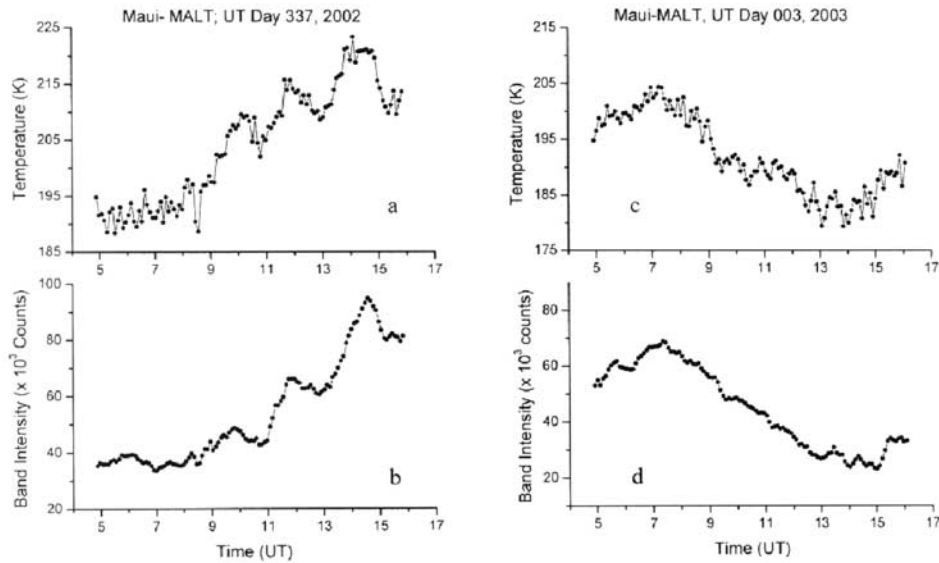
Figure 1. Temperature and intensity variations for O_2 emission for UT day 337, 2002 (left panel). A long period oscillation with embedded large amplitude shorter period oscillations are evident in the data while, the right panel show the variability for the UT day 003, 2003.

temperature and band emission intensity is evident. The temperatures increased significantly from ~190 K to ~220 K during the course of the night (data duration ~11-hrs). This ~30 K change represents a ~16% increase with respect to mean temperatures. The corresponding intensity data show a large ~90% change in intensity during the night. Superposed on this upward trend are several well-defined perturbations associated with a short periodicity (~2-hr) wave motion evident in both, the intensity and temperature (an analysis of this wave event is given later). In contrast, the right hand panel depicts a well defined long-period oscillation that exhibits a peak at ~0700 UT and a trough around 1400 UT suggesting a wave periodicity of ~12-hr. On this occasion the amplitude (peak-to-trough was ~20 K) and the associated intensity variation was ~ 78%. This example represents the maximum periodicity event that we have investigated using the available winter time data. Much smaller-scale variations (period ~1.4 hrs) are also evident in the data but, they are of low amplitude and are not investigated further in this report because of the accuracy of the instrument.

[7] To investigate the nature of the well-defined oscillations evident in the data, we first remove the large scale (unresolved) variability such as that evident as an upward trend in Figure 1a. Inspection of our MTM data set shows that the overwhelming majority of the nocturnal variation is dominated by long-period tidal features and therefore in this analysis, we have chosen to use a simple cosine model applied to the de-meaned data to determine the best-fit (least-squares) perturbation amplitude and periodicity assuming a tide-like perturbation of the form:

$$Y = A Cos\left[\pi \frac{(X - Xc)}{W}\right] \qquad (1)$$

where, A is the amplitude of the fitted wave of half-period W with phase Xc, and X is the time. The residuals are then

inspected for their quality and coherence. If their amplitude is significant (i.e. >4–5 K, well above the expected temperature uncertainties), they are then treated using the same formula to determine the amplitude and periodicity of the gravity wave.

[8] This analysis method applied to the data of Figures 1a and 1b is illustrated in Figure 2. The data (open squares) are plotted as variations about the mean value. The solid lines in both plots show the best fit cosine model results to these data. The fit to the temperature data (top panel) suggest a best fit wave periodicity of ~16 ± 1.2 hr with an amplitude of ~12.6 ± 0.6 K. A wave of the same periodicity was then
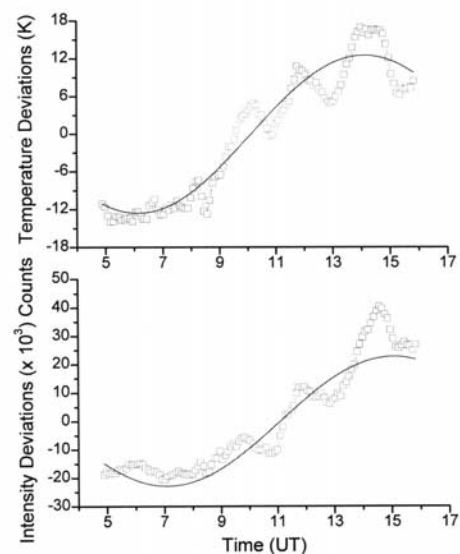

Figure 2. Simple sinusoidal best fit (solid lines in each plot) to the mean temperature and intensity deviations for the data shown in Figure 1.
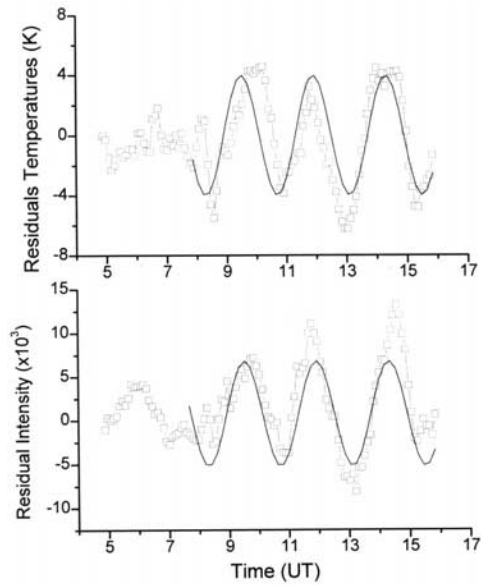
Figure 3. De-trended, residual mean temperature deviations for long period oscillations to signify the presence of short period oscillation in the data. Solid lines are the simple sinusoidal best fit model to the data.

Figure 4. Summary plot for our observed values for Krassovsky parameters. Solid lines represent a fourth order polynomial fit to the data.

successfully applied to the intensity data and the results of this fit are shown in the bottom panel. The MTM operates for solar depression angles $>12°$ providing typically 10–12 hrs data each night (wintertime) and observations of wave periodicities ~16 hrs are therefore not meaningful. However, the analysis has succeeded in de-trending the data and the residual temperatures, determined by subtracting from this long period oscillation, then provide meaningful information on the large amplitude, shorter-period oscillation evident in the data on this night.

[9] Figure 3 shows the residual temperature and intensity variations obtained after removing the upward trend evident in Figure 2 using this method. The top and bottom panel show residual temperature intensity variations respectively. An oscillation of ~2 hr periodicity clearly evident in both, the temperature and intensity data exhibiting ~3 cycles during the interval ~8–15 UT indicating a wave period of ~2 hrs. The oscillation appears to increase in amplitude with time; this is most evident in the intensity data where up to 4 cycles are seen. The residual temperature perturbations were then analyzed to determine a best fit wave periodicity and amplitude assuming a sinusoidal wave and using the model described by equation 1. The result of this simple wave fit to the data (solid curve) revealed the presence of 2.4 ± 0.3 hr wave with mean amplitude 4.1 ± 0.5 K. A similar analysis was then performed on the intensity residuals but using a wave of the same periodicity evident in the temperature data (2.4 hr). The results are indicated by the solid curve in the lower panel which shows a very good agreement in wave periodicity and depicts a mean wave amplitude perturbation of 10.2 (note, as the wave amplitude grew during the observation period and this is a conservative estimate of the intensity perturbation).

[10] Utilizing equation 1, the amplitude of the Krassovsky parameter for this wave event was then estimated to be 2.6 ± 0.8. To determine the phase relationship between the
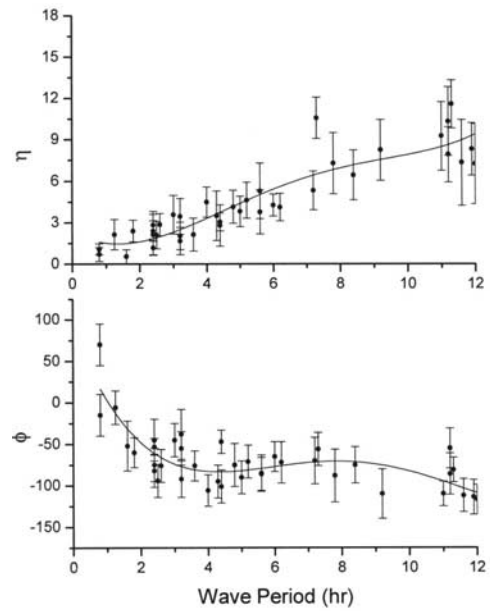
intensity and temperature waves, a cross correlation analysis was performed. Result reveals a well-defined correlation peak of ~0.95, when the temperatures were given a positive time shift of 0.4 ± 0.1 hr. This implies that the 2.4–hr wave in intensity led a phase shift $Ø = (0.4/2.4) \times 360 = 60° \pm 20°$ in associated temperature perturbation.

[11] Model studies of the O_2 emission by *Hickey et al.* [1993] have shown that 'η' is expected to vary significantly
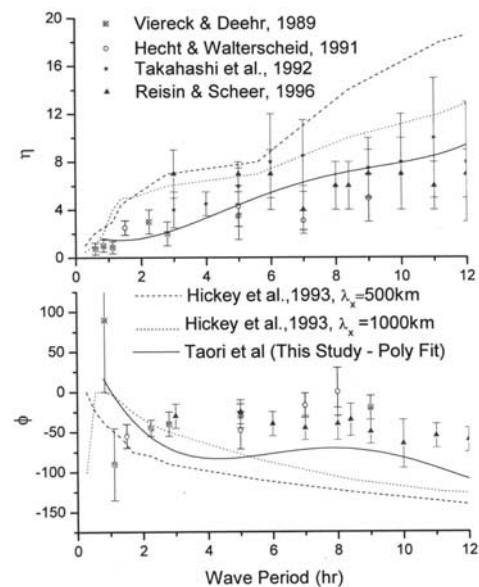

Figure 5. Comparison of our resultant polynomial fit (solid lines) with other similar measurements of Krassovsky analysis. Dashed and dotted lines represent the analytical model of *Hickey et al.* [1993] for 1000 and 500 km horizontal gravity wave wavelengths.

with season therefore, we restrict our analysis to winter-time data recorded from Maui during 2001–2003. A total of 17 nights of data containing 38 well-defined, coherent wave events were selected for this initial study. Each of these events exhibited significant wave amplitudes in both intensity and temperature and the results for $|\eta|$ and Ø are presented separately in Figure 4 for fitted wave periodicities ranging from 0.8–12 hrs (with the main emphasis on waves with apparent periods <6 hrs). In each case, the error bars indicated the uncertainty in our estimation of the magnitude and phase of η using this method of analysis.

3. Discussion

[12] Figure 5 compares our results with an ensemble of previous measurements of η reported in the literature. As mentioned earlier, there are relatively few available measurements of η and Ø for O_2 emission and we present here the composite results reported by *Viereck and Deehr* [1989], *Hecht and Walterscheid* [1991], *Takahashi et al.* [1992], and *Reisin and Scheer* [1996] together with their associated ranges. These measurements were obtained by ground-based instruments using similar techniques whereas the observations of *Zhang et al.* [1993] were from satellite and involved a significantly different method of determining η. To enable a clearer comparison of our results with these prior measurements we have plotted the two data curves (derived in Figure 5) together with the prior measurements and model predictions (dashed and dotted lines) of *Hickey et al.* [1993].

[13] $|\eta|$ comparison with the data ensemble (upper panel) show very good agreement in both, the magnitude of η and the apparent trend with increasing wave period. However, both our data and the previous measurements differ significantly in magnitude with the model prediction. Although, the model does show the same general trend for increasing η with observed wave period, there appears to be a substantial positive offset of ~3–6 compared with the model predictions for waves of horizontal wavelength in the range 500–1000 km.

[14] Comparison of our phase results with the data ensemble (lower panel) shows the same general trend for Ø to be approximately constant (for wave periodicities > 4 hrs) but, there appears to be a significant offset between our data curve (which represents the mean of our measurements) and the measurement ensemble, which suggests a somewhat smaller value for the phase shift of ~$-50°$ compared with our observed range of -70 to $-100°$. This said, our uncertainties in phase (not shown) range from ~10–$30°$ and thus within the limits of the measurements there is still considerable overlap with individual measurements comprising the data ensemble. Comparison with the model values (dashed and dotted lines) shows that our fitted curve agrees much better than the previously published data ensemble. In particular, the model results show a clear trend for the phase to decrease with wave period (over the range ~1–4 hrs) in reasonably good agreement with our observations. However, as the wave period increases, the model suggests somewhat higher negative values for phase than we have determined. At this point we note that our determinations of η and Ø for large wave periods (>8 hrs) are open to the discussion due to the finite data length but nevertheless our results agree

well with the other long – period observations reported here from the literature. In short, we expect best results for wave periodicities <8 hrs. Finally, it is interesting to note that the model values for 1000 km horizontal wavelengths are closer to the observed values, while one would expect the 500 km wavelength to be more realistic, especially for shorter period gravity waves. Coordinated measurements of Krassovsky parameters with all sky imaging photometers would put more light on these aspects.

[15] In summary, these measurements provide mixed results; agreeing well with the previously reported amplitude of η but, differ significantly in their associated phases. The model comparison further complicates the situation as our results agree better with model phases whereas the magnitudes are significantly less than the expectation. Referring to the recent work of *Hickey and Yu* [2005] on 'cancellation factor', and use of the same in gravity wave energy and momentum flux estimation in mesosphere using OH emission [*Swenson and Liu*, 1998], the results presented here in this report are of great importance and invites more studies and modeling work to understand the complex relationship that η comprises and its usages to study the mesospheric dynamics effectively.

References

Hecht, J. H., and R. L. Walterscheid (1991), Observation of the OH Meinel (6,2) and O_2 Atmospheric (0,1) nightglow emission from Maui during the ALOHA-90 campaign, *Geophys. Res. Lett.*, *18*, 1341–1344.

Hickey, M. P., and Y. Yu (2005), A full wave investigation of the use of a cancellation factor in gravity wave–OH airglow interaction studies, *J. Geophys. Res.*, *110*, A01301, doi:10.1029/2003JA010372.

Hickey, M. P., G. Schubert, and R. L. Walterscheid (1993), Gravity wave driven fluctuations in the O_2 atmospheric (0–1) nightglow from an extended, dissipative emission region, *J. Geophys. Res.*, *98*, 13,717–13,729.

Krassovsky, V. I. (1972), Infrasonic variations of OH emission in the upper atmosphere, *Ann. Geophys.*, *28*, 739–746.

Lowe, R. P., L. M. LeBlanc, and K. L. Gilbert (1996), WINDII/UARS observation of twilight behaviour of the hydroxyl airglow at mid latitude equinox, *J. Atmos. Terr. Phys.*, *58*, 1863–1869.

Reisin, E. R., and J. Scheer (1996), Characteristics of atmospheric waves in the tidal period range derived from zenith observations of O_2 (0–1) Atmospheric and OH (6–2) airglow at lower midlatitudes, *J. Geophys. Res.*, *101*, 21,223–21,232.

Swenson, G. R., and A. Z. Liu (1998), A model for calculating acoustic gravity wave energy and momentum flux in mesosphere from OH airglow, *Geophys. Res. Lett.*, *25*, 477–480.

Takahashi, H., P. P. Batista, Y. Sahai, and B. R. Clemesha (1985), Atmospheric wave propagations in the mesopause region observed by the OH (8,3) band, NaD, O_2A (8645 A) band and OI 5577 A emissions, *Planet. Space Sci.*, *33*, 381.

Takahashi, H., Y. Sahai, P. P. Batista, and B. R. Clemesha (1992), Atmospheric gravity wave effect on the airglow O_2 (0–1) and OH (9–4) band intensity and temperature variations observed from a low latitude station, *Adv. Space Res.*, *12*, (10)131–(10)134.

Tarasick, D. W., and G. G. Shepherd (1992a), Effects of gravity waves on complex airglow chemistries: 1. O_2 ($b^1\Sigma_g^+$) emission, *J. Geophys. Res.*, *97*, 3185–3193.

Tarasick, D. W., and G. G. Shepherd (1992b), Effects of gravity waves on complex airglow ehemistries: 2. OH emission, *J. Geophys. Res.*, *97*, 3195–3208.

Taylor, M. J., M. A. Hapgood, and P. Rothwell (1987), Observations of gravity wave propagation in the OI (557.7 nm), Na (589.2 nm) and the near infrared OH emissions, *Planet. Space Sci.*, *35*, 413.

Taylor, M. J., L. C. Gardner, and W. R. Pendleton Jr. (2001), Long period wave signatures in mesospheric OH Meinel (6,2) band intensity and rotational temperature at mid latitudes, *Adv. Space Res.*, *27*(6–7), 1171–1179.

Viereck, R. A., and C. S. Deehr (1989), On the interaction between gravity waves and the OH Meinel (6–2) and O_2 Atmospheric (0–1) bands in the polar night airglow, *J. Geophys. Res.*, *94*, 5397–5404.

Walterscheid, R. L., and G. Schubert (1995), A dynamical–chemical model of fluctuations in the OH airglow driven by migrating tides, stationary tides and planetary waves, *J. Geophys. Res.*, *100*, 17,443–17,449.

Zhang, S. P., R. N. Peterson, R. H. Wiens, and G. G. Shepherd (1993), Gravity waves from O_2 nightglow during the AIDA89 campaign I, Emission rate/temperature observations, *J. Atmos. Terr. Phys.*, *55*, 355–375.

_____

A. Taori, Aryabhatta Research Institute of Observational Sciences, Manora Peak, Naini Tal 263 129, India. (ataori@aries.ernet.in)

M. Taylor, Center for Atmospheric and Space Science, Utah State University, Logan, UT 84322, USA. (mtaylor@cc.usu.edu)